Hindawi
Journal of Spectroscopy
Volume 2018, Article ID 5120789, 11 pages
https://doi.org/10.1155/2018/5120789

Research Article

Using Compact ^{1}H NMR, NIR, and Raman Spectroscopy Combined with Multivariate Data Analysis to Monitor a Biocatalyzed Reaction in a Microreaction System

Robin Legner,[1,2] Alexander Wirtz,[2] and Martin Jaeger[2]

[1]*Department of Chemistry, University Duisburg-Essen, Universitaetsstraße 2, 45141 Essen, Germany*
[2]*Department of Chemistry and ILOC, Niederrhein University of Applied Sciences, Frankenring 20, 47798 Krefeld, Germany*

Correspondence should be addressed to Martin Jaeger; martin.jaeger@hs-niederrhein.de

Received 28 June 2018; Revised 19 September 2018; Accepted 14 October 2018; Published 2 December 2018

Academic Editor: Rizwan Hasan Khan

Process analytical technology aims at process knowledge and process improvement, efficiency, and sustainability. A prerequisite is process monitoring. The combination of microreaction systems and spectroscopy proved suitable due to dimension and compound reduction and real-time monitoring capabilities. Compact ^{1}H NMR, NIR, and Raman spectroscopy were used to monitor the biocatalyzed hydrolysis and esterification of acetic anhydride to isoamyl acetate using immobilized *Candida antarctica* lipase B (CALB) in a microreaction system in real-time. To facilitate the identification of signals suitable for the extraction of concentration-time (*c-t*) graphs, 2D heterocorrelation spectra were generated through covariance transformations applied to 1D Raman, NIR, and NMR data. By means of this purely mathematical statistical procedure, the relevant signals of the process media were assigned to educts and products and thus made applicable for univariate data evaluation. The data obtained were interpreted in terms of a first-order kinetic model, and corresponding reaction rate constants were extracted. An alternative, elegant, and fit-for-automation approach for the kinetic analysis of the spectra was demonstrated in using multivariate curve resolution (MCR). The results of the univariate and multivariate approaches were comparable with regard to reaction rates and concentrations. While the manual integration of the ^{1}H NMR spectra followed by univariate analysis allowed to establish a concentration profile of the final product isoamyl acetate hence revealing more details, multivariate analysis was found more suitable for process automation.

1. Introduction

Since the joint initiative of regulatory authorities and the pharmaceutical industry, process analytical technology (PAT) has evolved from a mere production support discipline into a fast-growing research area [1–3]. It has established itself as an important element of industrial production processes [4]. Thus, process analytical instruments are located in or nearby large-scale processes and reactors. Process understanding results from their application, which in fact is process monitoring. The process knowledge obtained aims at ensuring a constant final product quality. It further enables process control and allows process optimization. The process may be improved towards efficiency, hence cost reduction, sustainability, and safety [1, 2]. Meeting the customer demand for reproducible product quality is an important prerequisite for the competitiveness of a company, which requires using facilities, resources, and energy in the most economical way [5].

Today's process analytical tools comprise a variety of methodologies and take advantage of their inherent features [2]. Spectroscopy, spectrometry, and chromatography represent highly specific methods [4]. Among them, Raman and near-infrared (NIR) play major roles [6–8]. More recently, nuclear magnetic resonance (NMR) spectroscopy has grown into focus [9, 10]. During process monitoring, the information sought is most often the quantity of a compound at a given time. Therefore, spectroscopic techniques providing even relatively lower resolution and sensitivity than those commonly required for structure elucidation purposes satisfy the requirements for process monitoring. Process monitoring can proceed in-line, on-line, at-line or—less

desirable—off-line. For in-line monitoring, a probe is inserted into the reaction vessel. When the measurement is conducted on-line, a bypass is used. For at-line analysis, a sample is taken from the reaction and treated before analysis. Hence, in-, on-, and at-line monitoring types usually provide results in real-time [1, 2, 7, 11].

In order to compensate for the low resolution of, e.g., NIR or compact bench-top ^{1}H NMR spectrometers, suitable multivariate data analysis procedures have been devised and applied where univariate data processing did not prove sufficient [11–13]. Another strategy for enhancing spectral resolution has been developed by using covariance data processing [14–16]. This approach has been derived from statistical mathematics. Hence, different spectra that possess a common so-called perturbation dimension are correlated, where the spectral intensity represents a function of two independent variables such as wavenumber or frequency. This type of two-dimensional correlation spectroscopy has been introduced by Noda et al. for IR and also later for other vibrational and optical absorption methods [16–18]. For NMR spectroscopy, Brueschweiler et al. and Eads and Noda have reported on the use of covariance transformations to correlate frequency domains [19–21]. A 2D homocorrelation map is generated by transformation of a series of 1D spectra or a 2D spectrum from one spectroscopic technique. When two series of 1D spectra or two spectra of different spectroscopic techniques are correlated, a 2D heterocorrelation map results [22, 23]. Covariance methods are especially useful for the identification of spectral resonances suitable for process analysis.

Concentration-time (*c-t*) profiles from reaction monitoring can be obtained either by univariate methods or by multivariate methods such as the multivariate curve resolution alternating least squares (MCR-ALS) [24, 25]. Using this self-modelling curve resolution method, reaction kinetics can be determined directly from the recorded spectra series [26–28].

Isoamyl acetate belongs to flavoring substances, its odor being similar to both banana and pear. It is the main constituent of banana oil. Due to its odor, isoamyl acetate is used as artificial flavor [29, 30]. Its application as solvent and carrier, once known as aircraft dope, has vanished except for historical reproductions and scale models since airplanes are made of metal or carbon composites [31].

In this study, compact ^{1}H NMR, NIR, and Raman spectrometers were applied to monitor in real-time the biocatalyzed esterification to isoamyl acetate via the hydrolysis of acetic anhydride using immobilized *Candida antarctica* lipase B (CALB) in a microreaction system, cf. Scheme 1. The recorded spectra were transformed into 2D-heterocovariance correlation maps for the identification of specific resonances for univariate kinetic analysis. The results were compared to the kinetic parameters obtained from multivariate MCR-ALS analysis.

2. Theory

2.1. Multivariate Curve Resolution-Alternating Least Squares (MCR-ALS). Principal component nalysis (PCA) and partial least square regression (PLS-R) are among the most often used chemometric tools for process data analysis [32, 33]. Principal components and latent variables usually do not represent chemical and physical quantities. This is evenly true for the MCR-ALS algorithm. Physical-chemical knowledge on the process can be integrated into the chemometric analysis, as the number of components may be defined through the number of reactants and products [24, 25, 34]. From a data matrix $\mathbf{X}$ containing all spectral information as superpositions due to the reaction mixture, the information about the pure components, e.g., the spectra, can be extracted. In case of reaction monitoring, $\mathbf{X}$ represents spectral data. The data matrix can be decomposed into the small matrices $\mathbf{S}$ and $\mathbf{C}$ which consist of pure spectra and the associated concentration profiles and the residual matrix $\mathbf{E}$ as follows [25, 34–36]:

$$\mathbf{X} = \mathbf{C}\mathbf{S}^{\mathbf{T}} + \mathbf{E}. \tag{1}$$

The matrix $\mathbf{X}$ of dimensions $z \times s$ contains the recorded NMR spectra as rows with the respective intensity values. From reaction monitoring, spectral series represent a function of time. The transposed matrix $\mathbf{S}^{\mathbf{T}}$ of dimensions $a \times s$ contains the spectra of the pure components as rows a. In matrix $\mathbf{C}$ of dimensions $z \times a$, the contributions of the pure spectra in columns a correspond to the concentrations in the corresponding spectrum. The residual matrix $\mathbf{E}$ of dimensions $z \times s$ contains the spectral residues, which cannot be explained by the pure components. Residuals can represent random noise or systematic disturbances in the spectrum.

Matrices $\mathbf{C}$ and $\mathbf{S}$ can be computed by MCR-ALS. They are iteratively calculated from a first estimate for $\mathbf{C}$ or $\mathbf{S}$ in an alternating least-squares method as shown below [24, 35, 37]:

$$\hat{\mathbf{S}}^{\mathbf{T}} = \mathbf{C}^{+}\mathbf{X} = \left(\hat{\mathbf{C}}^{\mathbf{T}}\hat{\mathbf{C}}\right)^{-1}\hat{\mathbf{C}}^{\mathbf{T}}\mathbf{X}, \tag{2}$$

$$\hat{\mathbf{C}} = \mathbf{X}\mathbf{S}^{\mathbf{T}+} = \hat{\mathbf{S}}\mathbf{X}\left(\hat{\mathbf{S}}^{\mathbf{T}}\hat{\mathbf{S}}\right)^{-1}, \tag{3}$$

where $\wedge$ denotes the estimated value and + a pseudoinverse. The decomposition of $\mathbf{X}$ is achieved by iterative least-squares minimization of $\|\mathbf{E}\|$ under suitable constraints, i.e., a chemical kinetic model, nonnegativity in spectral, and concentration profiles as well as an initial guess of reagent and product concentrations. Since the uniqueness of the solution is determined by the secondary conditions, such as the chemical model, reaction order, and pure educt or product spectra, it is important to introduce as much physical-chemical knowledge of the system as possible into the constraints [34, 38].

2.2. Homo- and Heterocorrelation Spectroscopy. In contrast to NMR spectroscopy, vibrational spectroscopic techniques are not based on frequency pulse sequences that allow us to encode two frequency domains. While NMR spectroscopy is intimately associated with the Fourier transformation to generate 2D correlation spectra, a different approach was suggested by Eads and Noda and Frasinski et al. [21, 22, 39, 40] Covariance transformations were used to

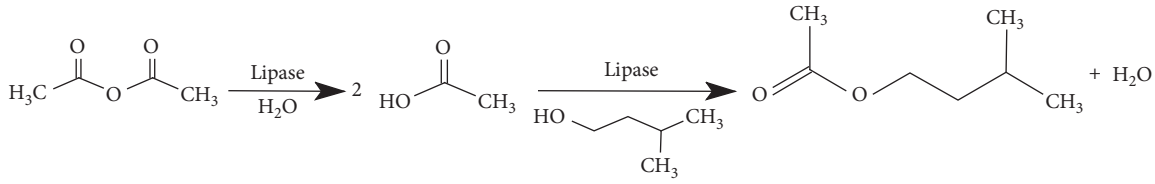

Scheme 1: Reaction scheme for the biocatalyzed hydrolysis of acetic anhydride followed by esterification with isoamyl alcohol to isoamyl acetate. Immobilized CALB catalyses both reaction steps as one-pot reaction in the microreaction system [29].

create a correlation map by recording one-dimensional spectra as responses to a quantitative, measurable perturbation applied to the sample in a systematic way [16, 18]. This perturbation may be temperature, pressure, concentration, stress, electrical field, and most importantly a chemical reaction [17, 41]. A correlation spectrum or map, $\mathbf{X}(\nu_1, \nu_2)$, is defined according to the following equation:

$$\mathbf{X}(\nu_1, \nu_2) = \langle \tilde{y}(\nu_1, t) \cdot \tilde{y}(\nu_2, t') \rangle, \quad (4)$$

where $\tilde{y}(\nu_1, t)$ is the spectrum affected by the perturbation, called the dynamic spectrum, and ν_1 and ν_2 are two different spectral variables at a given time or a fixed interval of the external variable t. The symbol $\langle\ \rangle$ denotes a suitable correlation function. The dynamic spectrum is computed by subtracting the average spectrum from each spectrum of a series of spectra. The quantitative comparison of spectral intensity variations can then be performed by means of statistical theory. Variations from a mean value are represented by covariances. Hence, the correlation map $\mathbf{X}(\nu_1, \nu_2)$ can be considered as the covariance matrix, when the series of dynamic spectra $\tilde{y}(\nu_1, t)$ is represented by a matrix. Assuming that $\mathbf{X}(\nu_1, \nu_2)$ is a complex number, it can be expressed according to the following equation consisting of the real part $\mathbf{\Phi}$ and the imaginary part $\mathbf{\Psi}$:

$$\mathbf{X}(\nu_1, \nu_2) = \mathbf{\Phi}(\nu_1, \nu_2) + i\mathbf{\Psi}(\nu_1, \nu_2). \quad (5)$$

For spectroscopic purposes, the relation between the covariance matrix and a spectrum, in particular 2D NMR spectra, was thoroughly proven [19, 20, 42]. The proof is based essentially on Parseval's theorem. The numerical calculation of the correlation maps has been described elsewhere [16, 20].

Due to the statistical nature of the approach, one series of spectra may be compared to another series of spectra originating from a different spectroscopic technique. This is referred to as heterocovariance spectroscopy [21, 41]. A heterocorrelation map will result according to the following equation:

$$\mathbf{X}(\mu_1, \nu_2) = \langle \tilde{x}(\mu_1, t) \cdot \tilde{y}(\nu_2, t') \rangle, \quad (6)$$

where μ_1 and ν_2 are the spectral variables from different spectroscopic techniques. Equation (6) can be rewritten in matrix notation, cf. Equation (7), where the square root is a consequence of Parseval's theorem [19, 20, 43]:

$$\mathbf{F} = \mathbf{C}^{1/2} = \left(\mathbf{S} \cdot \mathbf{G}^{\mathrm{T}}\right)^{1/2}, \quad (7)$$

where $\mathbf{F}$ is the 2D spectrum, $\mathbf{C}$ is the covariance matrix, and $\mathbf{S}$ and $\mathbf{G}$ are the two data matrices, such as a series of spectra with a common perturbation dimension. Cross-peaks in such correlation spectra have been reported as a help to disentangle crowded spectral regions [16, 43]. In this study, 2D heterocovariance correlation maps are computed from series of 1D ^{1}H NMR, Raman, and NIR spectra recorded during reaction monitoring.

3. Materials and Methods

3.1. Spectral Recording and Processing. NMR spectra were recorded on-line using a compact NMR picoSpin80 spectrometer with a proton Larmor frequency of 82 MHz (Thermo Fisher Scientific GmbH, Dreieich, Germany). It had a built-in flow cell and an electrical lock such that neat liquid process media were measured without further sample preparation or addition of deuterated solvents or reference standards. The sample cell possessed a total volume of 40 μL and an active volume of 40 nL. The operation temperature was 36°C. The spectrometer was controlled by Thermo Fisher PicoSpin software 0.9.3 running on the spectrometer control board and accessed via a web interface from a laptop computer. The free induction decay (FID) was recorded as 4092 data points that were zero filled to 8 k points prior to the Fourier transformation. The number of scans amounted to 16 and the pulse length was set to 60 μs corresponding to a 90° pulse. Spectra were recorded from 0.3 to 7 ppm. The bandwidth amounted to 4 kHz. All spectral processing was achieved through MestReNova 12.0.0 (Mestrelab Research S. L., Santiago de Compostela, Spain) on a laptop computer under Windows 7. The spectrum size after zero-filling and Fourier transformation (FT) resulted in 64 k. Pretreatment methods were used for spectra optimization. The spectra were binned with 0.004 ppm and normalized to the largest peak. Baseline correction was achieved using a Bernstein polynomial fit of 3rd order.

Raman spectra were recorded using the DXR™ SmartRaman spectrometer (Thermo Fisher Scientific GmbH, Dreieich, Germany) and processed using the Omnic software, version 9.2 (Thermo Fisher Scientific GmbH, Dreieich, Germany) running on a desktop PC under Windows 7. A Raman immersion probe from InPhotonics (InPhotonics, Inc., Norwood, MA, USA) was connected via a special module for fiber optics, allowing a distance between spectrometer and reaction vessel of up to 5 m. The probe was positioned at its focal point of 5 mm above the solution in the reaction vessel. Sixty-four spectra comprising a spectral range of 250–3500 cm^{-1} with a resolution of 5 cm^{-1} were acquired at each reaction time point. The laser was operated at 785 nm and 150 mW. For processing, the Omnic software

9.2 (Thermo Fisher Scientific GmbH, Dreieich, Germany) was used. During 1380 min, 50 spectra were recorded. All spectra were baseline corrected using an asymmetric 2nd order Huber function. The spectra were normalized to the highest band. For baseline correction and normalization, MatLab R 2017b (MathWorks, Inc., Natick, MA, USA) was used.

NIR measurements were carried out with the Antaris II FT-NIR Analyzer using the software Omnic, version 8.0 (Thermo Fisher Scientific GmbH, Dreieich, Germany). The spectral range was chosen from 4000–10000 cm^{-1} at a resolution of 4 cm^{-1} and the number of scans was set to 64. The spectrometer was equipped with a NIR transflection immersion probe Falcata (Hellma GmbH & Co. KG, Muellheim, Germany). All spectra were normalized after the baseline correction using an asymmetric Huber function 3rd order, again under MatLab R 2017b.

3.2. Microreaction Assembly. Stainless-steel microreaction components (Ehrfeld Mikroreaktionstechnik, Wendelsheim, Germany) were assembled according to Figure 1 [44, 45]. In an open storage vessel, the reactants, 20 mL of acetic anhydride (>98%, Merck KGaA, Darmstadt, Germany), 40 mL of isoamyl alcohol (>98%, Merck KGaA, Darmstadt, Germany), and traces of distilled water for the benefit of the enzyme, were mixed and transferred via a peristaltic pump Smartline 100 (Knauer GmbH, Berlin, Germany) into the microreaction assembly at a rate of 5 mL/min. The excess of isoamyl alcohol ensured complete conversion of the anhydride. Immobilization of the enzyme *Candida antarctica* lipase B (Novozymes A/S, Bagsvaerd, Denmark) was achieved by mixing the enzyme with the epoxy acrylate resin Purolite® ECR8205F (Purolite GmbH, Ratingen, Germany) in 50 mM phosphate buffer and stirring for 20 h at ambient temperature. The immobilized enzyme was then transferred into the cartridge of the Ehrfeld reactor F 200. The filled volume amounted to 1.8 of the 2 mL cartridge volume. The reaction was initiated through heating the reactor to 35°C. The residence time of a solution fraction, approximately 2 mL, in the reactor amounted to 2 min. The solution, then containing product, was recirculated into the storage vessel. The microreaction assembly was controlled through the software LabVision 2.10 (HiTec Zang GmbH, Herzogenrath, Germany).

The reaction mixture was diverted to the NMR spectrometer sample cell via a valve (Figure 1). Setting the valve, the flow was stopped after five seconds such that 16 spectra could be accumulated per sample. The following sample was introduced into the spectrometer via the bypass, transferring the previous one back to the vessel at the same time (cf. Figure 1). For Raman and NIR spectral recording, corresponding probes were attached a few millimeters above the surface of the reaction liquid in the storage vessel or was immersed into it (cf. Figure 2). The reaction was conducted over a period of 1380 min.

3.3. Covariance and Multivariate Data Analysis. The 2D correlation maps were generated using the program 2Dshige running on a personal computer under Microsoft Windows 7 [46]. Spectral data were exported as ASCII files from the spectral processing software listed above. To reduce the size of the data sets, 1D spectra were reduced by binning to 1 k data points for NMR, 732 data points for Raman, and 1 k data points for NIR. The data files were transformed into homo- or heterocorrelation maps and displayed as contour or color plots using appropriate threshold levels.

For MCR-ALS analysis, NMR, Raman, and NIR spectra were automatically imported into MatLab, version 2017b, wherein the MCR-ALS toolbox 2 was applied [35, 47]. Three latent variables or components were selected on the basis of visual inspection of the computational results. The non-negativity conditions for spectra and concentration profiles were set as constraints. Furthermore, a kinetic model A $\longrightarrow$ B was assumed. Other models tested were A $\longrightarrow$ B $\longrightarrow$ C and A + B $\longrightarrow$ C + D. It is noteworthy that the number of variables or components is not interchangeable with the number of real chemical components of the process system. An initial guess of the educt concentration ranged between 3.0 and 3.5 $mol \cdot L^{-1}$. As the starting value, the reaction rate constant was assumed to be $2.5 \cdot 10^{-3}$ min^{-1}. The agreement between calculated and experimental concentration-time profile was taken as goodness of the obtained kinetic parameters.

4. Results and Discussion

4.1. Qualitative Reaction Monitoring. The enzyme catalysed acetic anhydride hydrolysis, and subsequent esterification with isoamyl alcohol was conducted in a microreaction platform. The enzyme was immobilized and located in a cartridge reactor as a heterogeneous catalyst. The process was monitored using on-line 1D ^{1}H NMR and in-line Raman and NIR spectroscopy. Spectra were recorded during the course of the reaction over 1380 min. One aim of process analysis, process understanding, is represented here by generating *c-t* plots and their mathematical description using chemical kinetic theory. It is straightforward to seek educt or product specific signals in spectra, which can be interpreted in terms of concentrations. Starting with the interpretation of the NMR spectra, the usefulness of covariance spectroscopy, especially heterocorrelation spectroscopy shall be demonstrated. Yet, analysts more familiar with vibrational spectroscopy might start from Raman or NIR spectra as well. Relevant educt and product signals could be identified in ^{1}H NMR spectra (Figure 2).

The hydrolysis of acetic anhydride to free acetic acid appeared in the NMR spectrum through the methyl resonances at 2.0 and 1.8 ppm where the latter signal stems from acetic anhydride and the former from acetic acid. The following esterification reaction of free acetic acid with isoamyl alcohol to isoamyl acetate could be recognized by the very weak methyl resonance at 3.8 ppm. The water resonance, which was observed at 4.1 ppm at the beginning of the reaction, shifted in the course of the reaction and was found at 6.5 ppm by the end of the reaction. The signal migrated due to the change in the pH induced by the liberation of acetic acid. Due to the high selectivity of NMR spectroscopy, individual and well-separated signals could be attributed. This

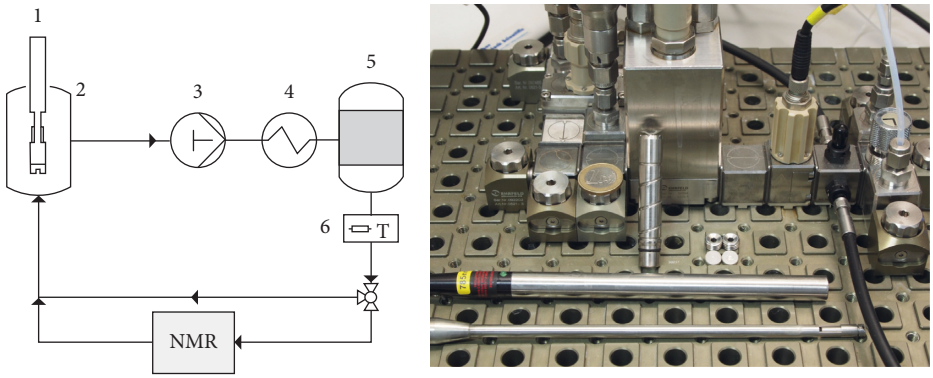

Figure 1: (a) Process flow-chart of the microreaction assembly: 1, Raman and NIR probe; 2, storage vessel containing the majority of the reaction mixture; 3, piston pump; 4, heat exchanger; 5, cartridge reactor; 6, temperature sensor; and then a compact ^{1}H NMR spectrometer is located in a bypass. (b) Picture of the microreaction platform (from left to right): inlet module, heat exchanger, cartridge reactor, T-sensor, optical flow cell, and outlet module. Raman probe and transflection NIR immersion probe (front).

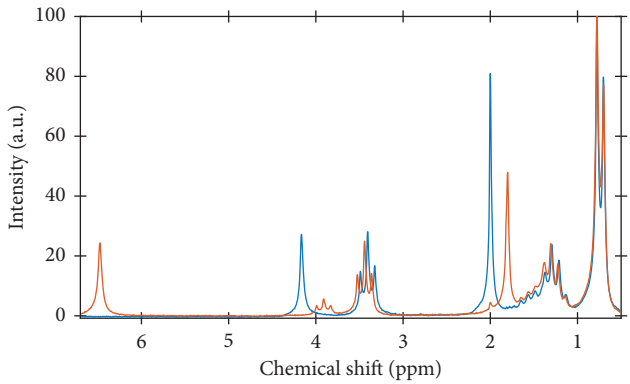

Figure 2: 1D ^{1}H NMR spectra of the biocatalyzed hydrolysis in the microreaction system. Spectrum at 0 min (blue) and at the end of process monitoring after 1380 min (brown).

is a prerequisite for the application of univariate data analysis. Hence, *c-t* curves were readily obtained for the reaction, (see Section 4.3).

While high resolution is intrinsic to high-field NMR spectrometers, the much smaller bench-top spectrometer operating at 82 MHz proton Larmor frequency provided sufficient resolution to obtain relevant educt and product bands. The following paragraph illustrates how the information gained from NMR analysis can be quickly transferred to Raman and NIR analyses.

4.2. 2D Correlation Spectroscopy to Support Reaction Monitoring. To easily discover signals or bands suitable for reaction monitoring, heterocorrelation maps were computed from NMR, Raman, and NIR spectra, as shown in Figure 3. Since spectral differences along with the reaction progress were most easily recognized and explained in ^{1}H NMR spectra, the gained information was transferred to the Raman and NIR spectra. While in other cases Raman or NIR spectrum prove more readily interpretable, the inverse approach works evenly well.

Heterocorrelation spectra do not contain diagonal peaks [16, 48]. Thus, all correlations observed related signal changes at a given NMR chemical shift to intensity changes at wavenumbers in Raman spectra. It is therefore by the sign of a correlation peak that educt and product signals can be attributed. Using selected successfully attributed NMR signals, i.e., 2.0 ppm for acetic anhydride, 3.8 ppm for isoamyl acetate, and 1.8 ppm for acetic acid, correlations with the bands at 800, 1700 and 1740, and 3000 cm^{-1} were observed (cf. Figure 3). In the region between 1740 and 1790 cm^{-1}, asymmetric and symmetric stretching vibrations of the two C=O groups of carboxylic acid anhydrides were detected. The product's methylene resonance at 3.8 ppm displayed only a very weak in-phase or positive correlation to the stretching C=O vibration from acetic acid at 1700 cm^{-1}. The positive sign is indicative for a product signal. The analogue applies for the correlations at 2.0 ppm, 2980 cm^{-1} and 1.8 ppm, 2980 cm^{-1}: The negative (blue) signal indicates an educt-product relationship, the positive (red) cross-peak a product-product one. In the range of 810–910 cm^{-1}, weak C-C stretching vibrations of acetates occurred. This signal was not directly apparent in the 1D Raman spectrum. Its counterpart however was visible in the NMR, which suggests that 2D correlation spectroscopy is also suitable for the identification of low-concentration byproducts [49].

The enzyme-catalysed hydrolysis of acetic anhydride could be followed through monitoring the C=O stretching vibration at 1740 cm^{-1} in Raman spectra and the methylene resonance in the range of 2.0 ppm in NMR spectra. The C=O stretching vibration displayed a negative correlation with the methylene resonance of acetic acid at 1.8 ppm, while the two educt and product signals run in opposite directions simultaneously. This is reflected by the positive correlations between 1740 cm^{-1} and 2.0 ppm, and between 1700 cm^{-1} and 1.8 ppm for the free acetic acid. Apart from a strong correlation in the range of the C-H vibrations at 3000 cm^{-1}, a moderate correlation in the range of 800 cm^{-1} from the substances involved in the hydrolysis could be recognized.

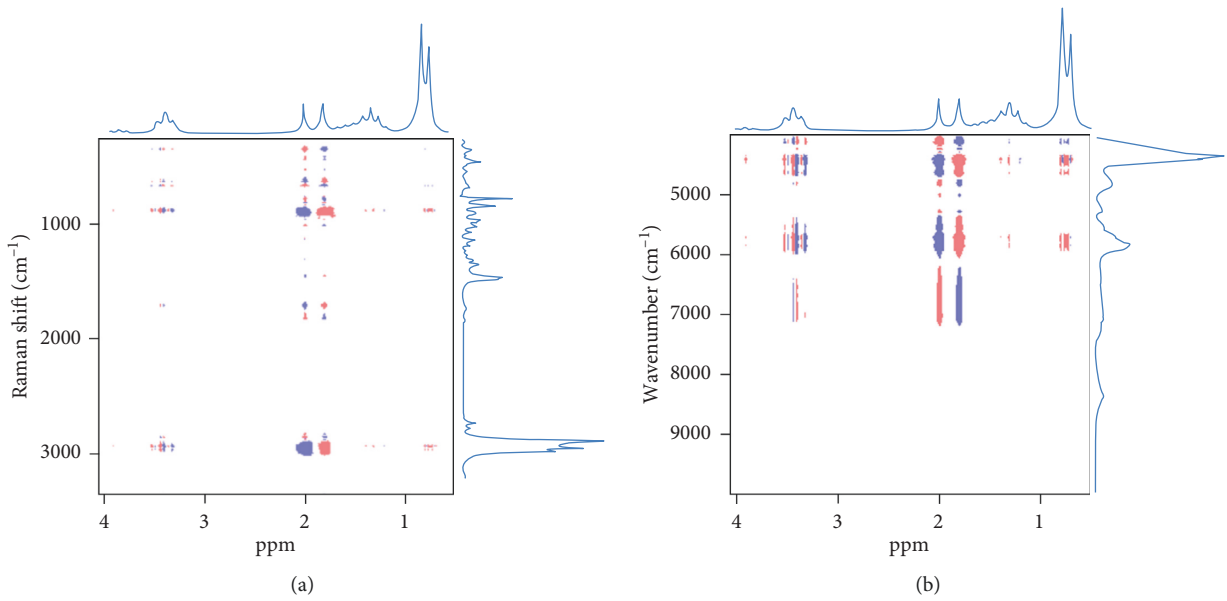

Figure 3: 2D ^{1}H NMR-Raman heterocorrelation spectra (a) of isoamyl acetate from immobilized lipase catalysis using in-line Raman spectroscopy (λ = 785 nm) and on-line 1D ^{1}H NMR. 2D ^{1}H NMR-NIR heterocorrelation map (b).

Firstly, a negative correlation of the acetic anhydride at 2.0 ppm resulted. Secondly, a positive correlation with the free acetic acid at 1.8 ppm was found [50].

In the ^{1}H NMR-NIR 2D heterocorrelation (cf. Figure 3(b)), signals reflecting the hydrolysis were observed, but a detailed assignment could not be achieved. Yet, from the 2D NMR-NIR correlation spectrum, the overtone and combination vibrations of C-H and O-H at 6250–7150 cm^{-1} and 4540–5000 cm^{-1} could be attributed by means of the respective positive and negative correlations to the methylene resonances at 2.0 and 1.8 ppm. It could also be recognized that a univariate evaluation would falsify the kinetic evaluation since observed bands represent superpositions of components [50].

In summary, the 2D heterocorrelation spectra helped to confirm the assignment of signals to an educt or a product by directly transferring the information from one spectroscopic technique to another. The 2D maps indicated the origin of vibrational bands from a single compound or as superposition. Heterocorrelation spectra were thus found to facilitate the identification and analysis of signals suitable for process monitoring. A selection of the 58 spectra recorded is shown in Figure 4 as stack plots for each spectroscopic method.

4.3. Quantitative Reaction Monitoring. Process analytics generally aims for the reception of concentration-time (*c-t*) data. Their extraction from spectra proceeded straightforward using the in-line and on-line monitoring at the microreaction assembly. Through spectral analysis using heterocovariance correlation plots, the signals corresponding to the educts and the product were identified as described above. Based on distinct signals, univariate analysis leading to *c-t* plots was applied. Nevertheless, series of spectra with the fully recorded spectral range were subjected to multivariate data analysis in the form of MCR-ALS.

Inspection of the NMR spectra (cf. Figure 4(a)) revealed that the water signal originating from the buffer system of the enzyme was well discernible. The spectra, in which the product signal was superimposed by the water shift, were discarded from kinetic evaluations. Since the area-under-the-curve of an NMR signal is proportional to the number of nuclear spins causing the signal, the actual relative concentration was determined by integrating the signals at 2.0, 1.8, and 3.8 ppm and by correcting them for the number of nuclei. To determine absolute concentrations, the internal standard method would need to be applied [51, 52]. Provided a sufficient linearity of the NMR amplifier, the absolute concentrations could be determined during the reaction since the initial concentrations of the reactants were known [51]. Due to nonlinearity of the amplifier, the relative composition of the mixture as obtained from direct integration of specific educt and product signals, hence univariate analysis, was plotted against reaction time (Figure 5).

While NMR spectra displayed a weak but interpretable signal of isoamyl acetate at 3.8 ppm, Raman and NIR spectra did not provide a corresponding band of sufficient intensity. Due to the choice of the process parameters, only a small amount of product was formed during the reaction period monitoring such that isoamyl ester product signals appeared weakly as seen by the NMR signal and its heterocorrelation at 3.8 ppm in the corresponding spectra. The first catalytic step, i.e., the hydrolysis of acetic anhydride to acetic acid, was monitored by the signals in the range of 2.0–1.8 ppm and the corresponding Raman band at 800 cm^{-1}. An acceleration of the reaction might be initiated by choosing a somewhat higher temperature. The esterification might occur eventually more prominent. The univariate evaluation of the signals from

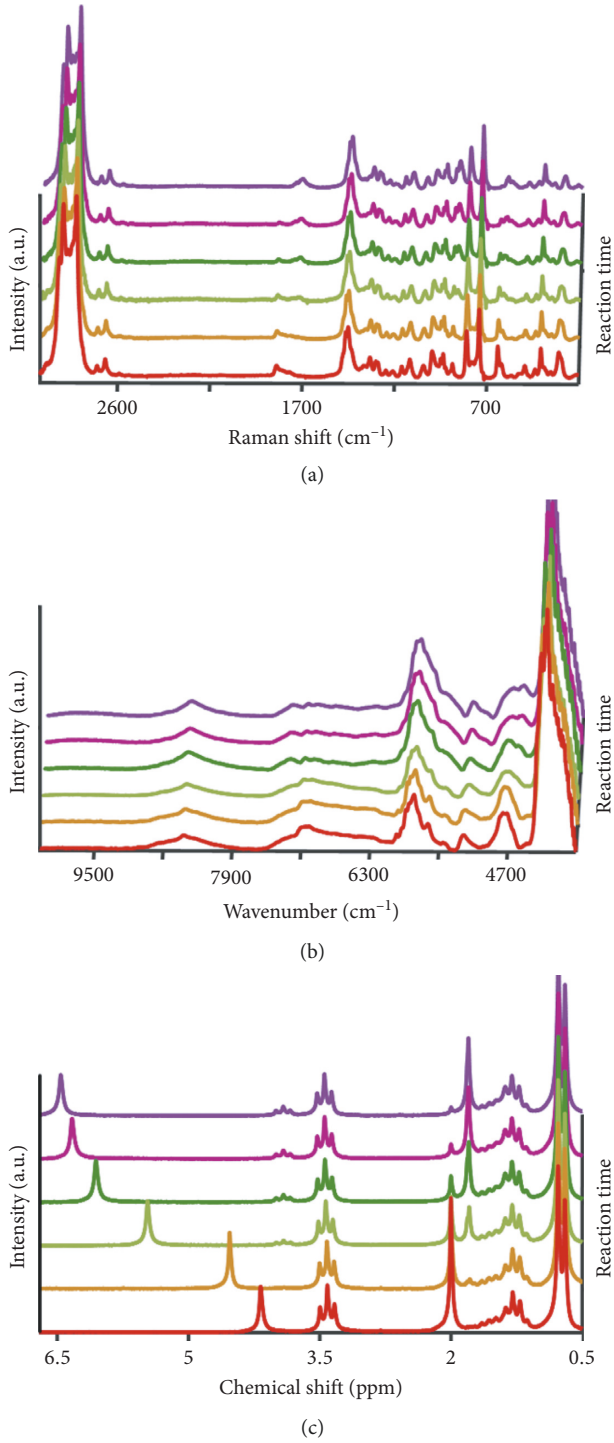

Figure 4: Raman (a), NIR (b), and ^{1}H NMR (c) spectra from on-line reaction monitoring of the enzyme catalysed reaction in the microreaction assembly. Spectra were recorded from the neat reaction mixture during 23 hours. NMR spectra, 16 accumulations, were acquired at 82 MHz and $T = 36^{\circ}$C. NIR spectra were recorded using an immersion probe. Raman spectra, 64 accumulations, were acquired with laser excitation at 785 nm. Color coding refers to corresponding reaction times among the spectroscopic methods. The reaction was followed over a period of 1380 min.

acetic acid and acetic anhydride yielded comparable reaction rate constants from Raman and NMR spectroscopic monitoring, showing the values of 2.1 and $2.2{\cdot}10^{-3}$ min^{-1} for the transformation from acetic anhydride to acetic acid (cf. Table 1). Within Raman spectra, the bands at 1740 and 1700 cm^{-1} were used for educt and product monitoring, respectively. A trial to use univariate analysis on NIR data did not give satisfactory results. While envisaging automation for process control, MCR-ALS analysis is seemed to be an attractive method as identification of suitable bands would not

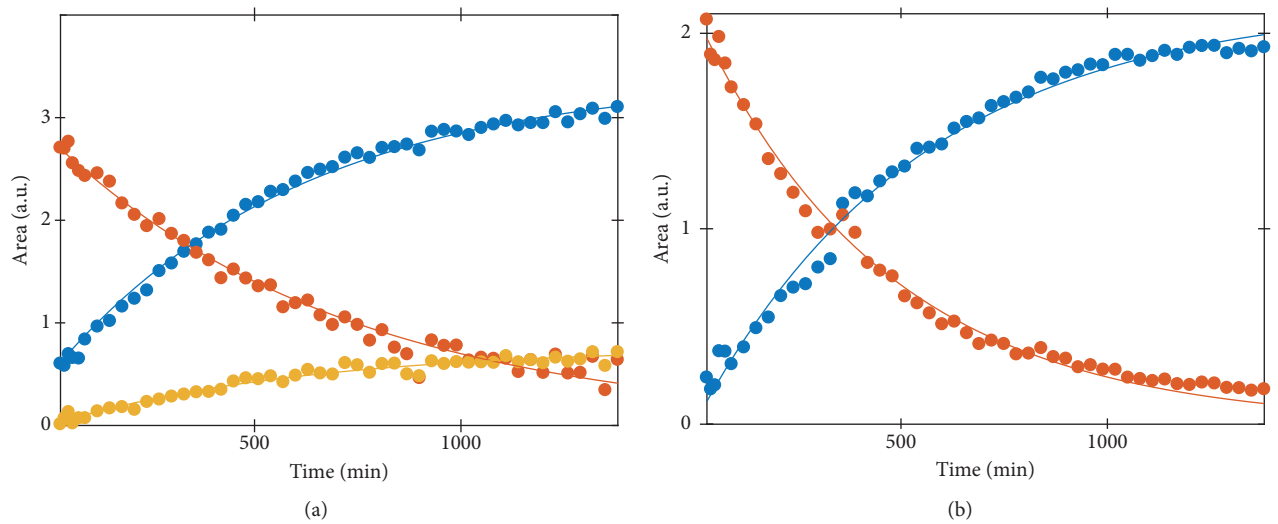

Figure 5: *c-t* plots as area-under-the-curve vs. time of the enzyme catalysed esterification from univariate data analysis and corresponding fits computed according to first-order reaction based on NMR (a) and Raman (b) spectra; acetic acid (blue), acetic anhydride (orange), and isoamyl acetate (yellow).

Table 1: Reaction order and rate constants according to ^{1}H NMR, Raman, and NIR spectroscopic methods for the enzyme-catalysed hydrolysis of acetic anhydride using univariate and multivariate spectral analyses.

	Univariate		Multivariate (MCR-ALS)	
	Reaction order	Rate constant ($min^{-1}\cdot10^{\cdot3}$)	Rate constant ($min^{-1}\cdot10^{-3}$)	Explained variance
^{1}H NMR	1	2.1	2.2	0.99
Raman	1	2.2	2.1	0.99
NIR	1	—	1.9	0.97

be required. The MCR-ALS analyses of NMR and Raman spectra are shown in Figure 6. Before computing the *c-t* curves, the first-order reaction mechanism, A ⟶ B, an initial guess of the rate constants, and the educt starting concentration were defined as boundary conditions [53].

The algorithm transforms spectral data into *c-t* data according to the predefined model, i.e., the first-order reaction. The correspondence of the extracted data to the model is visualized by the *c-t* curve. From Figure 6, it can be recognized that for Raman and NMR data, the agreement was very good. Only the NIR data did not prove of sufficient quality to yield good agreement to the model and thus minor scattering (cf. Figure 6(c)). The correspondence between *c-t* data and the first-order model was observed for all three spectroscopic techniques. Outliers, such as observed for the NIR analysis, may indicate disturbances, such as laboratory temperature change during sampling or measurement. Other reaction mechanisms were tested against the *c-t* data. Neither the second-order reaction A + B ⟶ C + D nor the follow-up reaction A ⟶ B ⟶ C displayed data fits with evenly good agreement as the first-order model. However, the low yield of the isoamyl acetate and therefore the resulting low signal-to-noise ratio influenced the performance of the algorithm so that no superior agreement with the models could be found.

Furthermore, the comparison of univariate to multivariate analyses showed a remarkable consistency with respect to the reaction order and the obtained rate constant. The results of the reaction monitoring of the enzymatic-catalysed hydrolysis reaction are summarized for univariate and multivariate analyses via MCR-ALS in Table 1.

All spectroscopic methods used revealed rate constants of a first-order chemical kinetic model. Because of enzyme catalysis, the reaction is likely to follow a pseudo-first-order mechanism, which would not be discernible from a first-order mechanism under the reaction conditions applied. Apparently, the catalysed hydrolysis proceeded faster or was preferred to the isoamyl ester formation. From univariate analysis of the NMR data (cf. Figure 5), a corresponding reaction constant of 1.3 10^{-3} min^{-1} was obtained. No multivariate description of this subsequent esterification could be achieved since isoamyl acetate was observed only in the NMR spectrum after about 2 hours of reaction time, provided careful visual inspection. It is assumed that the MCR-ALS algorithm was not able to identify isoamyl signals and—in case of Raman—bands that possessed a sufficient signal-to-noise ratio. The signal intensity of the product proved too low for the determination of a reasonable *c-t* profile through the MCR-ALS algorithm, whereas a trained analyst was able to extract consistent data. Thus, the univariate data analysis offered in this case the advantage to quantify extremely small signals, which also requires a greater effort for the evaluation.

The enzyme is also known to suffer from acid pH which was a consequence of the formation of acetic acid. The pH of the process solution dropped below the working range of the biocatalyst of pH 5–9. It was hence assumed that the CALB lost activity and ceased to produce isoamyl acetate. As a consequence, the subsequent reaction would not significantly affect the determined rate constants.

It should be noted that the intensity of vibrational bands depends on oscillator strength and polarizability, which is in

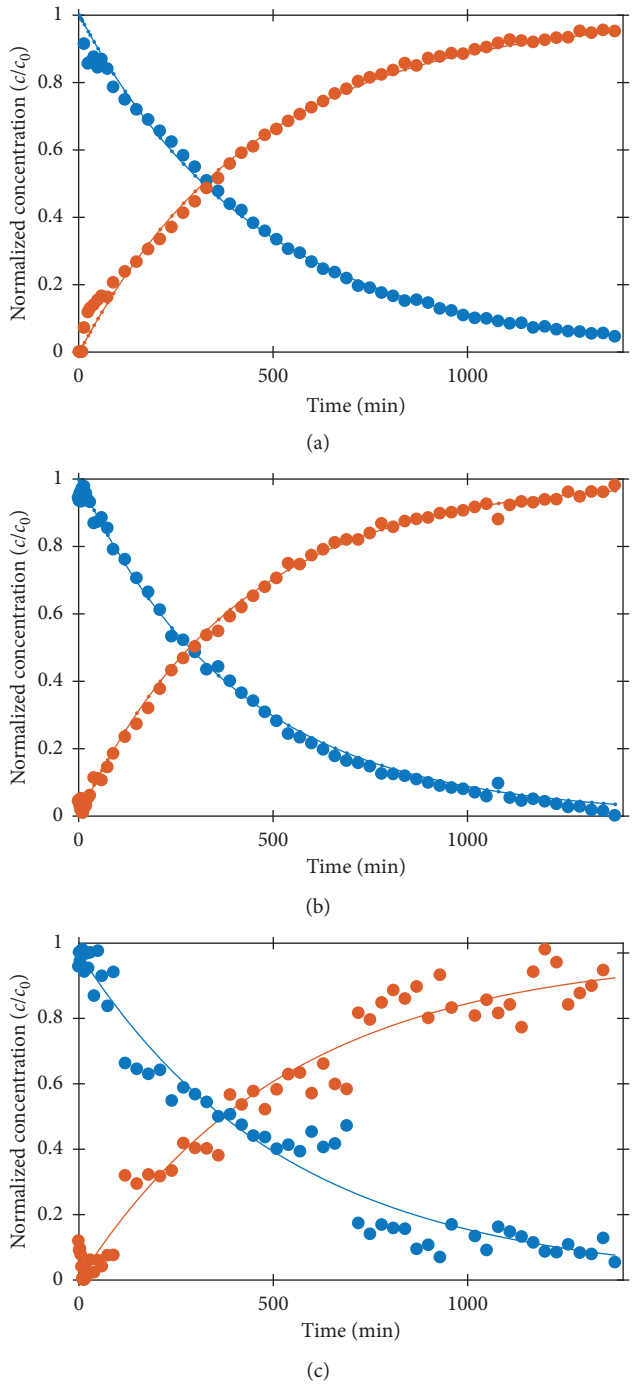

Figure 6: *c-t* profiles from MCR-ALS modelling for the enzyme-catalysed hydrolysis of acetic anhydride to acetic acid in the Ehrfeld microreaction system. Results on the basis of the ^{1}H NMR (a), Raman (b), and NIR (c) data. The computed data fits correspond to first-order reaction A ⟶ B (orange and blue lines), and the points are extracted data for product (red) and educt (blue).

general different for two different bands. Thus, the actual concentrations or concentration ratios of products and educts could not be derived from the Raman bands in contrast to the NMR resonances.

In summary, two approaches may be followed to obtain *c-t* data, which proved fit for process analytical technology: univariate analysis and MCR-ALS as a multivariate approach. Covariance spectroscopy, here in the form of heterocorrelation spectroscopy, was suitable to help identify specific signals of educts and products. Fundamental process understanding could be achieved through describing the *c-t* curves using kinetic models. Starting from the mathematical description of the data, it becomes possible to predict the course of the reaction and to quickly recognize deviations from the expected process. This knowledge may then be used to automate process control.

5. Conclusions

Analytical bench-top instruments, i.e., a compact ^{1}H NMR operating at 82 MHz, NIR and a Raman spectrometer, were successfully combined with a stainless-steel microreaction assembly. The CALB catalysed hydrolysis, and subsequent esterification of acetic anhydride to isoamyl acetate served as model for a heterogeneous biocatalysis reaction. NMR spectra provided distinct signals of all educts and the product, and NIR and Raman bands could not easily be assigned on visual inspection of the spectra. To facilitate the assignments, 2D heterocorrelation maps were computed from series of 1D NMR and 1D vibrational spectroscopic data using covariance transformations.

Quantitative analysis of the spectroscopic data was achieved using univariate and multivariate methods. The *c-t* data obtained from NMR, Raman, and NIR proved of sufficient quality to test a first-order or pseudofirst-order kinetic model yielding consistent results. The MCR-ALS algorithm was applied successfully for a biocatalyzed reaction. Yet, an improved signal-to-noise ratio, e.g., through increasing the number of acquisitions but thus prolongation of the measurement time, will enhance the recognition of low-abundant species. Furthermore, the MCR-ALS algorithm may be simultaneously applied to the data of the three analytical techniques. The knowledge on the process obtained by spectroscopic monitoring, heterocorrelation-based spectral interpretation, and univariate or multivariate kinetic analysis may allow future process control. For automation purposes, MCR-ALS was judged better suitable than univariate data treatment. Educt feed, reaction temperature, and flow rate should be optimized for best yields. These process parameters may then be adjusted automatically by detecting deviations from the corresponding reaction kinetics and counteracting through a feedback loop.

Data Availability

Data were recorded on NMR, Raman, and NIR spectrometers from Thermo Fisher Scientific. The raw data can be provided in the spectrometer file format. Data have been analyzed using MatLab. MatLab files can be obtained upon request from the corresponding author. Upon request, we can also include a link to download from the cloud Sciebo.

Conflicts of Interest

The authors declare that there are no conflicts of interest regarding the publication of this article.

Acknowledgments

The authors are grateful to Thermo Fisher Scientific for the vibrational and nuclear magnetic resonance spectrometers within a SEED project and A. Nickisch-Hartfiel and P. Naderwitz for technical and bio-technological expertise. R.L is very grateful for a grant from the German Academic Scholarship Foundation. The authors thank the Niederrhein University of Applied Sciences (HSNR) for financial support.

References

[1] United States Food and Drug Administration, *Guidance for Industry: PAT—A Framework for Innovative Pharmaceutical Development, Manufacturing, and Quality Assurance*, U.S. Department of Health and Human Services, Washington, DC, USA, 2004.

[2] European Medicines Agency, *Reflection Paper: Chemical, Pharmaceutical and Biological Information to be Included in Dossiers when Process Analytical Technology (PAT) is Employed*, European Medicines Agency, Canary Wharf, London, UK, 2006.

[3] K. A. Bakeev, *Process Analytical Technology*, John Weiley & Sons Ltd, Chichester, England, 2nd edition, 2010.

[4] W. Chew and P. Sharratt, "Trends in process analytical technology," *Analytical Methods*, vol. 2, no. 10, pp. 1412–1438, 2010.

[5] A. Chanda, A. M. Daly, D. A. Foley et al., "Industry perspectives on process analytical technology: tools and applications in API development," *Organic Process Research & Development*, vol. 19, no. 1, pp. 63–83, 2014.

[6] R. J. A. Do Nascimento, G. R. De Macedo, E. S. Dos Santos, and J. A. De Oliveira, "Real time and in situ near-infrared spectroscopy (NIRS) for quantitative monitoring of biomass, glucose, ethanol and glycerine concentrations in an alcoholic fermentation," *Brazilian Journal of Chemical Engineering*, vol. 34, no. 2, pp. 459–468, 2017.

[7] R. Schalk, F. Braun, R. Frank et al., "Non-contact Raman spectroscopy for in-line monitoring of glucose and ethanol during yeast fermentations," *Bioprocess and Biosystems Engineering*, vol. 40, no. 10, pp. 1519–1527, 2017.

[8] K. Dégardin, A. Guillemain, and Y. Roggo, "Comprehensive study of a handheld Raman spectrometer for the analysis of counterfeit medicines," *Journal of Spectroscopy*, vol. 2017, Article ID 3154035, 13 pages, 2017.

[9] B. Blümich and K. Singh, "Desktop NMR and its applications from materials science to organic chemistry," *Angewandte Chemie International Edition*, vol. 57, no. 24, pp. 2–17, 2017.

[10] M. F. Isaac-Lam, "Determination of alcohol content in alcoholic beverages using 45 MHz benchtop NMR spectrometer," *International Journal of Spectroscopy*, vol. 2016, Article ID 2526946, 8 pages, 2016.

[11] S. Kern, K. Meyer, S. Guhl et al., "Online low-field NMR spectroscopy for process control of an industrial lithiation reaction—automated data analysis," *Analytical and Bioanalytical Chemistry*, vol. 410, no. 14, pp. 3349–3360, 2018.

[12] F. Dalitz, M. Cudaj, M. Maiwald, and G. Guthausen, "Process and reaction monitoring by low-field NMR spectroscopy," *Progress in Nuclear Magnetic Resonance Spectroscopy*, vol. 60, pp. 52–70, 2012.

[13] N. Zientek, C. Laurain, K. Meyer, M. Kraume, G. Guthausen, and M. Maiwald, "Simultaneous 19F–1H medium resolution NMR spectroscopy for online reaction monitoring," *Journal of Magnetic Resonance*, vol. 249, pp. 53–62, 2014.

[14] D. A. Snyder, R. Bruschweiler, G.E. Morris, and J.W. Emsley, "Multidimensional correlation spectroscopy by covariance NMR," in *Multidimensional NMR Methods for the Solution State*, John Wiley & Sons Ltd, Chichester, UK, pp. 97–105, 2009.

[15] M. Jaeger and R. L. E. G. Aspers, "Covariance NMR and Small Molecule Applications," *Annual Reports on NMR Spectroscopy*, vol. 83, pp. 271–349, 2014.

[16] I. Noda, A. E. Dowrey, C. Marcott, G. M. Story, and Y. Ozaki, "Generalized two-dimensional correlation spectroscopy," *Applied Spectroscopy*, vol. 54, no. 7, pp. 236A–248A, 2000.

[17] I. Noda, "Generalized two-dimensional correlation method applicable to infrared, Raman, and other types of spectroscopy," *Applied Spectroscopy*, vol. 47, no. 9, pp. 1329–1336, 1993.

[18] I. Noda, "Two-dimensional infrared spectroscopy," *Journal of the American Chemical Society*, vol. 111, no. 21, pp. 8116–8118, 1989.

[19] N. Trbovic, S. Smirnov, F. Zhang, and R. Brüschweiler, "Covariance NMR spectroscopy by singular value decomposition," *Journal of Magnetic Resonance*, vol. 171, no. 2, pp. 277–283, 2004.

[20] R. Brüschweiler, "Theory of covariance nuclear magnetic resonance spectroscopy," *Journal of Chemical Physics*, vol. 121, no. 1, pp. 409–414, 2004.

[21] C. D. Eads and I. Noda, "Generalized correlation NMR spectroscopy," *Journal of the American Chemical Society*, vol. 124, no. 6, pp. 1111–1118, 2002.

[22] L. J. Frasinski, K. Codling, and P. A. Hatherly, "Covariance mapping: a correlation method applied to multiphoton multiple ionization," *Science*, vol. 246, no. 4933, pp. 1029–1031, 1989.

[23] I. Noda, "Modified two-dimensional correlation spectra for streamlined determination of sequential order of intensity variations," *Journal of Molecular Structure*, vol. 1124, pp. 197–206, 2016.

[24] L. R. Terra, M. N. Catrinck, and R. F. Teófilo, "MCR-ALS applied to the quantification of the 5-hydroxymethylfurfural using UV spectra: study of catalytic process employing experimental design," *Chemometrics and Intelligent Laboratory Systems*, vol. 167, pp. 132–138, 2017.

[25] W. Kessler and R. W. Kessler, "Multivariate curve resolution: a method of evaluating the kinetics of biotechnological reactions," *Analytical and Bioanalytical Chemistry*, vol. 384, no. 5, pp. 1087–1095, 2006.

[26] Y. Le Dréau, N. Dupuy, J. Artaud, D. Ollivier, and J. Kister, "Infrared study of aging of edible oils by oxidative spectroscopic index and MCR-ALS chemometric method," *Talanta*, vol. 77, no. 5, pp. 1748–1756, 2009.

[27] R. Tauler, "Multivariate curve resolution applied to second order data," *Chemometrics and Intelligent Laboratory Systems*, vol. 30, no. 1, pp. 133–146, 1995.

[28] R. J. Pell and X. Chen, "Multivariate curve resolution for understanding complex reactions," *Journal of Chemometrics*, vol. 28, no. 5, pp. 411–419, 2014.

[29] A. Güvenç, N. Kapucu, and Ü. Mehmetoğlu, "The production of isoamyl acetate using immobilized lipases in a solvent-free system," *Process Biochemistry*, vol. 38, no. 3, pp. 379–386, 2002.

[30] F. W. Welsh, W. D. Murray, R. E. Williams, and I. Katz, "Microbiological and enzymatic production of flavor and fragrance chemicals," *Critical Reviews in Biotechnology*, vol. 9, no. 2, pp. 105–169, 1989.

[31] C. H. Dickinson, J. Watson, and B. Wallace, "An impression method for examining epiphytic micro-organisms and its

application to phylloplane studies," *Transactions of the British Mycological Society*, vol. 63, no. 3, pp. 616–619, 1974.

[32] Z. P. Chen, J. Morris, A. Borissova et al., "On-line monitoring of batch cooling crystallization of organic compounds using ATR-FTIR spectroscopy coupled with an advanced calibration method," *Chemometrics and Intelligent Laboratory Systems*, vol. 96, no. 1, pp. 49–58, 2009.

[33] G. Mazarevica, J. Diewok, J. R. Baena, E. Rosenberg, and B. Lendl, "On-line fermentation monitoring by mid-infrared spectroscopy," *Applied Spectroscopy*, vol. 58, no. 7, pp. 804–810, 2004.

[34] W. Kessler and R. W. Kessler, "Multivariate curve resolution—integration von Wissen in chemometrische modelle," *Chemie Ingenieur Technik*, vol. 82, no. 4, pp. 441–451, 2010.

[35] J. Jaumot, N. Escaja, R. Gargallo, C. González, E. Pedroso, and R. Tauler, "Multivariate curve resolution: a powerful tool for the analysis of conformational transitions in nucleic acids," *Nucleic Acids Research*, vol. 30, no. 17, p. 92e, 2002.

[36] R. Tauler, "Multivariate curve Resolution : theory and applications," *Trends in Analytical Chemistry*, vol. 23, pp. 70–79, 2004.

[37] W. Kessler, *Multivariate Datenanalyse für die Pharma-, Bio- und Prozessanalytik*, Wiley-VCH, Weinheim, Germany, 2006.

[38] A. L. Pomerantsev and O. Y. Rodionova, "Process analytical technology: a critical view of the chemometricians," *Journal of Chemometrics*, vol. 26, no. 6, pp. 299–310, 2012.

[39] L. J. Frasinski, A. J. Giles, P. A. Hatherly, J. H. Posthumus, M. R. Thompson, and K. Codling, "Covariance mapping and triple coincidence techniques applied to multielectron dissociative ionization," *Journal of Electron Spectroscopy and Related Phenomena*, vol. 79, pp. 367–371, 1996.

[40] R. L. E. G. Aspers, P. E. T. J. Geutjes, M. Honing, and M. Jaeger, "Using indirect covariance processing for structure elucidation of small molecules in cases of spectral crowding," *Magnetic Resonance in Chemistry*, vol. 49, no. 7, pp. 425–436, 2011.

[41] M. Jaeger and R. Legner, "Homo- and hetero-covariance NMR spectroscopy and applications to process analytical technology," in *Spectroscopic Analyses—Developments and Applications*, E. Sharmin and F. Zafar, Eds., pp. 55–80, 2017.

[42] B. W. Hu, P. Zhou, I. Noda, and G. Z. Zhao, "An NMR approach applicable to biomolecular structure characterization," *Analytical Chemistry*, vol. 77, no. 23, pp. 7534–7538, 2005.

[43] B. Hu, J. P. Amoureux, and J. Trebosc, "Indirect covariance NMR spectroscopy of through-bond homo-nuclear correlations for quadrupolar nuclei in solids under high-resolution," *Solid State Nuclear Magnetic Resonance*, vol. 31, no. 4, pp. 163–168, 2007.

[44] W. Ehrfeld, V. Hessel, and H. Loewe, "Microreactors—new technology for modern chemistry," *Organic Process Research & Development*, vol. 5, no. 1, p. 89, 2001.

[45] R. Legner, S. Häfner, M. Voigt et al., "Micro process analytical technology—monitoring chemical processes in microreactors using miniature spectrometers," *GIT*, vol. 3-4, pp. 38–40, 2016.

[46] S. Morita, *2Dshige (c)*, Kwansei-Gakuin University, Nishinomiya, Japan, 2004-2005.

[47] J. Jaumot, A. de Juan, and R. Tauler, "MCR-ALS GUI 2.0: new features and applications," *Chemometrics and Intelligent Laboratory Systems*, vol. 140, pp. 1–12, 2015.

[48] Y. Mee Jung and I. Noda, "New approaches to generalized two—dimensional correlation spectroscopy and its applications," *Applied Spectroscopy Reviews*, vol. 41, no. 5, pp. 515–547, 2006.

[49] I. Noda, "Progress in two-dimensional (2D) correlation spectroscopy," *Journal of Molecular Structure*, vol. 799, no. 1–3, pp. 2–15, 2006.

[50] G. Socrates, *Infrared and Raman Characteristic Group Frequencies*, John Wiley & Sons Ltd., Chichester, UK, 3rd edition, 2004.

[51] G. Wider and L. Dreier, "Measuring protein concentrations by NMR spectroscopy," *Journal of the American Chemical Society*, vol. 128, no. 8, pp. 2571–2576, 2006.

[52] F. Malz and H. Jancke, "Validation of quantitative NMR," *Journal of Pharmaceutical and Biomedical Analysis*, vol. 38, no. 5, pp. 813–823, 2005.

[53] N. Viereck, L. Nørgaard, R. Bro, and S. B. Engelsen, "Chemometric analysis of NMR data," *Modern Magnetic Resonance*, pp. 1833–1843, 2008.